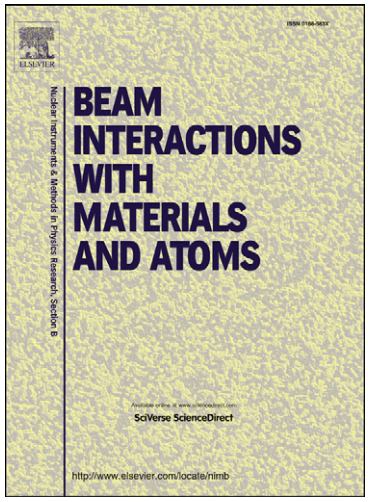

Millimeter length micromachining using a heavy ion nuclear microprobe with standard magnetic scanning

F. Nesprías, M.E. Debray, J. Davidson, A.J. Kreiner, N. Vega, E. de la Fournière

PII: S0168-583X(13)00239-5
DOI: http://dx.doi.org/10.1016/j.nimb.2013.02.009
Reference: NIMB 59303

To appear in: *Nucl. Instr. and Meth. in Phys. Res. B*

Received Date: 19 December 2012

Please cite this article as: F. Nesprías, M.E. Debray, J. Davidson, A.J. Kreiner, N. Vega, E. de la Fournière, Millimeter length micromachining using a heavy ion nuclear microprobe with standard magnetic scanning, *Nucl. Instr. and Meth. in Phys. Res. B* (2013), doi: http://dx.doi.org/10.1016/j.nimb.2013.02.009

Millimeter length micromachining using a heavy ion nuclear microprobe with standard magnetic scanning

F. Nesprías[1], M.E. Debray[1,2,*], J. Davidson[1,3], A.J. Kreiner[1,2,3], N.Vega[1] and E. de la Fournière[1]

[1] *Gerencia de Investigación y Aplicaciones, Comisión Nacional de Energía Atómica, Av. Gral Paz 1499 (1650), San Martín, Buenos Aires, Argentina.*

[2] *Escuela de Ciencia y Tecnología. Universidad Nacional de Gral. San Martín, M. De Irigoyen 3100 (1650), San Martín, Buenos Aires, Argentina.*

[3] *CONICET, Avda. Rivadavia 1917(C1033AAJ), Ciudad Autónoma de Buenos Aires, Argentina.*

Abstract

In order to increase the scanning length of our microprobe, we have developed an irradiation procedure suitable for use in any nuclear microprobe, extending at least up to 400% the length of our heavy ion direct writing facility using standard magnetic exploration. Although this method is limited to patterns of a few millimeters in only one direction, it is useful for the manufacture of curved waveguides, optical devices such Mach-Zehnder modulators, directional couplers as well as channels for micro-fluidic applications. As an example, this technique was applied to the fabrication of 3mm 3D-Mach-Zehnder modulators in lithium niobate with short Y input/output branches and long shaped parallel-capacitor control electrodes. To extend and improve the quality of the machined structures we developed new scanning control software in LabView™ platform. The new code supports an external dose normalization, electrostatic beam blanking and is capable of scanning figures at 16 bit resolution using a National Instruments™ PCI-6731 High-Speed I/O card. A deep and vertical micromachining process using swift ^{35}Cl ions 70 MeV bombarding energy and direct write patterning was performed on $LiNbO_3$, a material which exhibits a strong natural anisotropy to conventional etching. The micromachined structures show the feasibility of this method for manufacturing micro-fluidic channels as well.

Key Words: Direct write, Swift heavy ions, Lithium Niobate, Wave guides

* Corresponding author. Tel.: +54-11-67727068; Fax +54-11-67727121

Email address: debray@tandar.cnea.gov.ar (M. E. Debray)

1. Introduction

Focused MeV ion beams have provided a way to develop high resolution lithography. The direct-write micro-machining using MeV ion beam energies has been significantly developed since its inception for more than a decade [1]. Most of the effort of direct write technology using MeV protons beams known as proton beam writing (PBW) [2], was concentrated on reducing the beam size and the fabrication of high density and high aspect ratio structures with very smooth walls and tens of nanometers in size in polymer resists [3,4]. This has been achieved by using very stable accelerators with high brilliance ion sources, development of new magnetic focusing lenses and a detailed study of those parameters that affect beam focusing such as intrinsic aberrations, misalignment of magnetic focusing lenses, collimator slits scattering, etc. PBW has been used in the nano-machining of a wide range of materials with several applications [5, 6].

However, in many cases in the manufacture of devices is necessary which some of the characteristic lengths of a structure have micro or nanometers sizes, while other lengths have scales some orders of magnitude higher (mm or cm). This is the case of optical devices and micro-channels for applications in micro-optics and micro-fluidics.

In almost all nuclear microprobes the beam is scanned over the resist in a digitized pattern using a set of orthogonal magnetic scan coils. The intrinsic problem of the nuclear microprobes is the limited size of the fabricated structures, since the magnetic rigidity of MeV ions greatly restricts the achievable scan areas.

To overcome this restriction, during the last few years different methods have been developed to extend the capability of PBW to the production of long structures. One of these, denominated “synchronized line-scanning”, which utilizes a sophisticated combination of

magnetic and stage scanning was applied to the fabrication of micro-photonics and fluidics devices with more than one centimeter in length [7, 8].

Recently, a very simple method using a static proton beam was applied to produce up to 8 mm length uniformly-irradiated straight lines in semiconductors and polymers [9]. This method is attractive by its simplicity, and can be used with any nuclear microprobe. Although this approach is ideal for producing straight linear structures of several millimeters in length, it can not be used for the manufacture of devices which include curved shapes, such as MZ modulators or micro-fluidic circuits.

In contrast to the extensive use of proton beams, the use of swift heavy ions for beam writing is scarce due to the very small number of facilities that can accelerate and focus heavier ions with tens of MeV energy to micrometer dimensions [10 – 13].

Although heavy ions, with the same energy per nucleon (MeV/AMU) are more difficult to focus to sub/micrometer dimensions and have lower penetration ranges, they transfer to the material a bigger amount of energy per unit of length than lighter ions as protons or alpha particles. For example, a ^{35}Cl beam at 70 MeV with a current density of only 1ppA/μm^2 deposits in lithium niobate approximately 5.4 MW/cm^3.

It is this ability to transfer a huge energy density in a very short time and in a very small volume causing physical and chemical changes with unique features, which allows us to use heavy ions with few MeV/AMU to extend direct writing to more radiation hard materials, defining for the heavy ion nuclear microprobes niche application areas in which they do not compete with PBW [14].

Since the magnetic deflection depends on momentum/q, with q the charge of the ion, the magnetic scanning becomes more problematic in swift heavy ion microprobes.

One of the major problems involved in the production of waveguides or micro-channels by heavy ion beam writing in a hard radiation material as $LiNbO_3$, is the limitation caused by the

magnetic rigidity which constrains the magnetic scanning to at most a few hundred of microns. In contrast, a 2 MeV proton beam from a standard proton microprobe can cover up to 2x2mm^2 [15]. Therefore, while a heavy ion microprobe is able to focus a wide range of different MeV/AMU ions to micron and sub-micron beam spot sizes, the magnetic rigidity of the swift heavy ions limits the maximum scan area.

This document describes the irradiation procedure to obtain a few millimeter length prototypes using a heavy ion microprobe with standard magnetic scan and, as examples of the ability of the method, the fabrication of micro-channels and 3D optical waveguides in lithium niobate.

2. Experimental Setup

We have successfully used high energy (70 MeV) $^{35}Cl^{6+}$ beams from the Tandar Laboratory Heavy-ion Microbeam (MiP) facility to perform the micro-machining of 3D-structures in $LiNbO_3$ using a direct write process [14].

The MiP comprises an OM55 (Oxford Microbeams design) high strength magnetic quadrupole triplet lens system capable of focusing high energy heavy ions up to around 160 MeV.amu/q^2, a scanning system with a ferrite cored magnetic box deflector and a dual channel power amplifier (OM-40e). The standard scanning system (OMDAQ) raster scans the beam over the sample with a maximum resolution of 256x256 pixels. As known from previous work [1, 16], this scan method imposes restrictions for high resolution micromachining of complex shapes.

In the manufacture of direct write micro-machined curved shapes, such as those required for a Mach-Zehnder interferometer or micro-fluidic channels, a high resolution scanning system is essential in order to produce well defined smooth structures.

Rather than describing the method to extend the micro-machining length, we will describe the development and application of a new scanning system specifically designed for our heavy ion direct write process.

3. New scanning control and blanking

Taking into account the first version of the program *Ionscan* [17], we have developed a new scanning control system optimized for direct high energy ion beam writing. The new control system called Hiscan (Heavy-ion scan) uses a National Instruments™ PCI-6731 High-Speed 16Bits I/O card controlled by a code written in a LabView™ platform. The program generates the scan pattern and controls many of the tasks which are performed during the writing process: 1) Magnetic scan coils, which move the beam on the sample and make the figure patterns, 2) Beam blanking plates, which allow deflection of the beam on demand, 3) Dose normalization using X-ray detection, 4) XYZ stage, which moves the sample in the three coordinate axes.

Scan resolution of the new system can be set up to 65536 x 65536 pixels (16Bits resolution) and an update time of 1μs. In addition, the raster scan mode has been replaced by a scanning vector algorithm allowing the development of very smooth curves and avoiding the "serrated" edges [14], characteristic of the old simple matrix scan.

A beam switch is set right between the object and divergence angle defining slits. It consists of two 15cm long parallel metal sheets with a 4mm gap. The conducting layers are made of thin copper foils laminated onto a non-conductive substrate using printed circuit board technology. They are mounted in the beam-line about 5m from the experimental chamber. The blanker is needed to prevent the beam hitting the sample during its relocation to the next position and is used to switch the beam on and off in order to control that the preset number of ions irradiates the target. The blanker deflects the beam away from the aperture slits for a

preset time interval or the beam can be removed / restored on demand between independent forms of a complex structure, by following a predetermined automatic sequence. Also, the switch can be used to reduce the beam current in very low dose experiments as IBIC, changing the duty-cycle of the applied signal.

A high voltage amplifier (Technisches Büro Fisher, Ober-Ramstadt, Germany) triggered by a TTL signal produced by the scanning program on demand, releases a ±440V pulse to the plates within 320ns. The plates are charged with different polarity in order to increase the blanking speed. Compared to the usual dwell time per pixel, the blanker removes the beam very fast.

The parameters that characterize a given scanning pattern, as in the case of the MZ modulator: the width of the guide, the overall length, the transition length in the longitudinal direction, the distance between the parallel arms and their lengths are specified by an Excel™ spreadsheet. The program calculates all values required for vector scanning: radii, branching angles, start and end points of straight lines, etc.

One very important aspect for the micromachining of the MZ modulator is to maximize the ability of the new scanning system to produce guide contours with the highest possible finishing quality. In order to achieve this, the scanning pattern of MZ was split into three parts: bottom, top and center as shown in Fig. 1.

Each part was specified by a file that contains up to a maximum of 10^4 points [18]. For a MZ 1 mm long, each point or pixel corresponds to 0.14 μm steps for the central part and 0.11 μm steps for the bottom and top shapes. For a 3mm length MZ, each of these steps becomes three times longer, however, remaining well below the used ~ 3μm beam size. This relationship still ensures a smooth scanning.

The design includes also six more different rectangular parts. Four are the electrical contacts for wire-bonding (two, for each arm of the modulator) and two more at the input and output of

the device. These rectangular areas do not require a high quality surface finishing and were machined (in the horizontal direction) with a lower resolution setting of approximately 0.7um and 2.1μm by step for modulators with lengths of 1 mm and 3 mm respectively.

4. Methodology and beam optical simulations.

The magnetic deflector is made up of a box-shaped ferrite core whose XY orthogonal coils are arranged in such a way that each couple of opposing coils generates orthogonal dipole fields on the mid-planes of the system parallel to the axis of the coils [see 15]. Because the triplet quadrupole focusing system has different demagnifications and hence different deflection sensitivity in each plane (x and y planes), the coils in one direction are larger than in the orthogonal set. Normally the scanning systems are installed so that the smaller coils deflect in the low demagnification plane and are connected to the fast scan output of the scanning system. With this arrangement, the smaller scanning coils move the beam faster in the plane of high deflection sensitivity, while in the plane of low deflection sensitivity the scan coils generate the stronger field.

Since Tandar is a vertical accelerator, the focusing(F)-defocusing(D) capabilities of the high excitation Oxford triplet lens system are FDF in the vertical plane (high demagnification / low sensitivity scanning plane) and DFD in the horizontal plane (low demagnification / high sensitivity scanning plane).

In our system we have rotated the position of the scan coils so that the larger coils deflect the beam in the low demagnification plane. With the scanning system calibrated (following the procedure described in reference [15]) on both axes perpendicular to the beam direction, the largest area that can be scanned with a focused $^{35}Cl^{6+}$ beam at 70MeV energy (approximately 68 MeV.amu/q^2) is about 0.85x0.85mm^2.

Fig.2 shows an overlap of PRAM (Propagate Rays and Aberrations by Matricies code) [19, 20] simulations of single ion trajectories with maximal $\phi_{X,max} \sim \pm 150$ μrad divergences in the horizontal and vertical planes. The asymmetry in the trajectories in both planes is due to the deviation of chloride ions caused by the magnetic fields of the scanning coils. The field values correspond to the maximum scanning length that can be achieved with a square calibrated scanning system, which is less than 1 mm for both planes. Note in Fig. 2 that the lateral extent of the $\phi_{X,max} \sim -150$μrad divergence beam trajectory in the low demagnification plane, has almost the same value as the bore radius when it passes through the second focusing lens. The bore radius for the lenses of our high demagnification heavy ion microprobe is 3.75 mm.

The procedure to extend the scanning range of the focused heavy ion beams consists in using the magnetic scanning coils rotated 90^o and working with non-square scanned areas. The original calibration is preserved in the y-plane, but not in the x-plane. In this way, it was possible to extend the scanning range in the x-plane up to 4 times more than with the square scanning condition and obtain curved patterns up to 3.5mm length. This is achieved just in the plane in which at the same time the scanning coils have greater deflection sensitivity and the triplet lowest demagnification capability. In the orthogonal plane, the scanning coils are less sensitive (half number of turns), the triplet demagnification limits the deflection and the scan amplifier work at full gain (maximum calibration setting), making it impossible to extend the scan range (see Fig. 2). Clearly, the rotation of the scanning coils limits the maximum attainable length in the vertical plane, but allows a significant extension in the horizontal plane.

Breaking the square calibration generates the disadvantage that the figures with curved shapes could result in distorted micromachining patterns. This distortion can be overcome deforming the original pattern of the figure in such a way, that it accurately compensates the stretching produced during the magnetic scan.

As an example of this procedure, this paper shows the fabrication of a 3D MZ interferometer shape with micro-machined sidewalls. The extensive side channels are also shown in this work, as samples of potential applications in micro-fluidics.

Waveguide bend is a basic building block for waveguide devices. In the case of a MZ modulator, the most critical parts in the micromachining process are the Y-split input and the Y-coupling output. In Fig. 4, we show the comparison between the two methods most often used to make Y-branches and the distortion produced by a scan stretched by a factor three. The first corresponds to a cosine shape, which preserves its functional form after stretching. The stretching only readjusts the argument of the cosine function, resulting in an elongated cosine S-bend shape. The second is an S-shape made of two circular arcs with a constant radius of curvature. In this case, although the stretching modifies the original functional form (the curvature radius is no longer constant), for a stretching factor 3 this change is 1.73% in the region of greatest deviation and only 0.73% on average. In any case, the resulting S-bend is so close to the exact form that the MZ pattern can be made without correcting the stretching deformation.

It is also important to consider the maximum horizontal displacement of the beam passing through the lens pipe. Note the PRAM simulation in Fig. 3, the lateral displacement of the beam with divergences between $-150\mu rad \leq \Phi_X \leq 75\mu rad$ is greater than this, and only the trajectories with divergences between $75\mu rad \leq \Phi_X < 150\mu rad$ exit the lens tube and reach the sample. Hence, if the magnetic dipole field of the big coils is increasing starting from the situation showed in Fig. 2, the most extreme trajectories in the low demagnification plane ($\phi_X \sim -150\mu rad$) start hitting the wall of the lens pipe, reducing the total current reaching the point focus. The reduction of the beam current limits the length of the written structures, because it is not possible to achieve the necessary dose to produce the subsequent chemical etching.

Assuming a uniform current density passing through the aperture collimator in the example of Fig. 3, only a quarter of the total current is reaching the sample.

It follows from the above discussion that the limitation on the maximum attainable scan size is given by the radius of the tube. As mentioned, the radius of the output pipe of our heavy ion microprobe is only 3.75 mm and the maximum scan size is close to this value. It is interesting to mention that in a standard proton microprobe having a radius of 7.5mm it would be possible to achieve by this method magnetic scan lengths up to 7 mm.

4. Experimental procedure

The lithium niobate used in this work was of the x-cut type with 2mm thickness. The $LiNbO_3$ wafers were cut into approximately 0.5x1cm2 samples using a diamond circular saw, cleaned with solvents and ultrasonic agitation and washed with de-ionized water. After this process the samples were covered with an evaporated deposit of Cu (~ 2.4μm). The micromachining of LiNbO3 was made using 35Cl beams at 70MeV energy, in vacuum, at room temperature and with the samples positioned almost normal to the beam direction. After passing through the Cu coating, the exit energy of the 35Cl ions is approximately 44.1 MeV. For this ion energy, the electronic stopping power at the lithium niobate surface is about 6.8 MeV/μm (calculated with the SRIM2006 code), which is well above the Se ≈ 5 MeV/μm threshold for continuous track formation [21]. A more complete description of the fabrication process used in this work can be found in [14].

In our pelletron accelerator [22], the intensity fluctuation of the ion beam during the fabrication is inevitable and can result in insufficiently irradiated crystal areas. In our irradiations we have tried to minimize this problem by averaging the dose in each pixel, scanning the beam repeatedly over the shape to reach the desired fluence value before proceeding to the next shape. As discussed later, this approach may be changed by the pixel

normalization to extend the micromachining length. Between shapes, the beam is deflected by the beam blanker. The minimum exposure dose for $^{35}Cl^{6+}$ ions with energies above the 5MeV lithium niobate threshold for continuous track formation is required to be $5x10^{12}$ ions/cm^2 [14]. Due to the possible beam current fluctuations occurring during the writing process a 10^{13} ions/cm^2 higher exposure dose was applied, which is sufficient to prevent possible unexposed areas.

The dose is controlled using an 80 mm^2 SDD (Ketek GmbH, VITUS Vacuum SDD) detector positioned very close to the sample (~ 1cm) to take advantage of the large inner shell ionization induced by swift heavy ions and the associated X-ray production.

The measurement of the stretching as function of the X-scan size was done as follows: with the beam properly focused and the scan size calibrated on both planes, a segment of 850μm length was written along the horizontal axis on a PMMA sheet. Increasing the X-scan size, the beam was scanned to create an array of segments with different lengths, each one of them for every calibration value. In each case, the length of the footprint left by the beam on the PMMA was measured on-line, using the micrometer head of the translation sample stage. These values were verified through irradiations on lithium niobate and measurements by means of light microscopy after etching. While the stretching increases proportionally to the scan size value of the scanning amplifier, it was not possible to exceed the maximum elongation of approximately 3 mm, which correspond to the setting value 8 in the scale of the x-calibration control of the OM-40e scan amplifier. As discussed above, for setting values between 8 and 10, the micromachining length can not be increased due to the current loss by the collision of the beam with the lens pipe. With the new non-square size “calibration”, we proceeded to perform the direct write of the MZ patterns on lithium niobate.

The development of the latent $LiNbO_3$ image after the ion exposure was made using hydrofluoric acid solution (50%) wet etching at room temperature.

The effect on the developed structures is shown in Fig. 5, in which the machined line using average dose normalization is diluting as the beam is reaching the ends. This represents a difficulty for the machining of very sensitive materials, because if the scanning time is increased so that the ends receive the required dose, the central region of the structure will be overexposed. Although micromachining is diluted at the ends, this dose difference between the center and the ends of the pattern does not cause appreciable deterioration of the quality of the rest of the structure in lithium niobate, which has a very wide dose window (2.5×10^{12} – 2.5×10^{13} Cl–ions/cm^2). For the machining of most sensitive resist materials this problem can be corrected increasing the dose at the ends of the scan using pixel normalization.

Since our $LiNbO_3$ samples are covered with a thin Cu coating with the purpose to avoid the up-charging of the resist during the irradiation and to establish the fluence (number of ions/cm^2) through the measurement of the Cu $K_{\alpha,\beta}$ X-ray production, we took advantage of this method to measure the change in X-ray yield along the scan. This yield is proportional to the beam current and hence, to the fluence.

Fig. 6 shows the X-ray yield for both scanning methods: average and pixel normalization. In the first, the x-ray intensity falls to zero at the extremes of the scan, which as mentioned, is related to the reduction of the beam intensity due to the scattering with the beam pipe as the magnetic field of the horizontal scan coils increases during the scan. Moreover, with the pixel normalization the X-ray intensity remains uniform along the scan, ensuring that there is a more even distribution of fluence along the written structure.

As a result of the correction of the fluence by pixel-normalization, the machined line was extended approximately 250 um at each end, as it is shown in Fig. 5. In this way, it can extend the overall length of the structures to a maximum of approximately 3.5 mm. The length was measured for the normalized pixel segment, which has well-defined edges. The pixel normalization method has the disadvantage that the dwell time per pixel at the ends can be

very long, especially when the intensity of the x-ray falls to almost zero. However, if one is not interested in producing many structures as fast as possible but some prototypes as long as possible, this is an acceptable solution. The effectiveness of a combination of average and normalization pixel in which each pixel is delivered to only a percentage of the total dose and the beam is scanned several times over the sample to achieve the total fluence remains to be tested. Since the normalization per pixel gives the correct length of a given micro-machining segment, the calibration process described previously using pixel normalization was performed again.

With the beam focused, it is possible to create groups of modulators simply repeating the irradiation iteratively at different locations on the sample by changing the starting point of the magnetic scanning. In our system, from 850 to 1000 μm extension (depending upon the magnetic rigidity of the ion) available in the vertical direction, only a central region of about 400 to 500 μm is usable with good resolution. Outside, the beam resolution degrades progressively. In addition, it is also possible to generate structure arrays (of groups) by moving the sample orthogonally to the beam scanning direction. Fig. 7 shows an array of groups of three modulators of 1, 2 and 3 mm lengths produced with a 70MeV $^{35}Cl^{6+}$ beam, using a current of about 10 pA and a fluence of approximately 10^{13} ions/cm^2 in $LiNbO_3$. The scanning frequency was 10^3 pixel/s, and the time needed to irradiate a 3mm length MZ total pattern was approximately 900s.

Fig. 8 a) shows in more detail the parallel arms of the MZ and the regions of electrical contacts. The reader can note the difference in the step resolution used in each case and it can be seen (Fig. 8 b) that the beam resolution is lower in the x-axis (scanning axis), resulting in a small widening (decrease the width of the guide) in the curved sections. The 3D MZ modulators with the side channels are shown only as examples of the machining lengths possibilities, but still have not been optically characterized.

5. Conclusions

In conclusion, we have developed a new method to extend up to approximately 4 times the length of the magnetic scanning of our heavy ion microprobe. This is achieved by transposing the scanning coils and abandoning the squared size calibration. Although, this method is limited to large patterns of a few millimeters length in only one direction, it is useful for the manufacture of curved waveguides, optical devices such MZ modulators, directional couplers as well as channels for micro-fluidic applications.

Furthermore we have developed and implemented new heavy ion beam scanning vector software (HiScan). This code allows the micromachining of one or more arbitrary shapes up to 16 bit scan resolution. The current version enables the beam blanking and dose normalization control. Shape and pixel normalization can be used. The latter has been used to extend the length of the micro-machined figures. Currently, the dose normalization is performed with PIXE on an evaporated Cu coating of the sample. The code also has the ability to drive a new xyz sample stage.

Furthermore, with this method and the new vector scanning code we have successfully fabricated in lithium niobate (using a 70 MeV energy $^{35}Cl^{6+}$ beam) 3D shape Mach-Zehnder modulators and channels up to 3.5 mm length. Results do not show a deterioration in the beam resolution at the scanning ends, at least, for the about 3 μm beam resolution used in this work.

Another important feature is that, it is simple, easy to implement and applicable to any nuclear microprobe. The machinable length limitation is imposed by the bore diameter of the focusing lens pipe. Although it is not the same setup used in this work (in our system, the configuration of the quadrupole lenses is just right for a vertical machine), probably with a simple rotation of the focusing configuration it should be possible to make very long scans, particularly in standard proton microprobes where the pipe lens diameter is 15mm.

The results also show that this technique is ideal for the rapid prototyping of micro-fluidic and optical circuits of millimeter lengths and arbitrary design in $LiNbO_3$. Future versions of the software will incorporate the ability to perform combined stage and magnetic scanning [8] for the fabrication of long waveguides and micro-fluidic channels as long as 2 cms.

References

[1] S.V. Springham, T. Osipowicz, J.L. Sanchez, L.H. Gan, F. Watt, Nuc. Instr. And Meth. B 130 (1997) 155.

[2] F. Watt, M. B. H. Breese, A. A. Bettiol and J.A. van Kan, Materials Today Vol.10 (2007) 20-29.

[3] J.A. van Kan, T.C. Sum, T. Osipowicz and F. Watt, Nuc. Instr. And Meth. B 161-163 (2000) 366.

[4] J.A. van Kan, A.A. Bettiol, F. Watt, Appl. Phys. Lett. 83 (2003) 1629

[5] S. Bolhuis, J.A. van Kan and F. Watt, Nuc. Instr. And Meth. B 267 (2009) 2302

[6] J.A. van Kan, A.A. Bettiol and F. Watt, Nuc. Instr. And Meth. B 260 (2007) 396

[7] L.P. Wang, P.G.Shao, J.A. van Kan, K. Ansari, A.A. Bettiol, X.T. Pan, T. Wohland and F. Watt, Nucl. Instrum. and Meth B260 (2007)450-454.

[8] C. Udalagama, E.J. Teo, S.F. Chan, V.S. Kumar, A.A. Bettiol and F. Watt, Nucl. Instrum. and Meth. B269, (2011)2417-2421, 12th International Conference on Nuclear Microprobe Technology and Applications.

[9] B.Q. Xiong, M.B.H. Breese, S. Azimi, Y.S. Ow and E.J. Teo, Nucl. Instrum. and Meth. B269 (2011)729–732

[10] M. Varašanec, I. Bogdanović Radović, Z̆. Pastuović, M. Jakšić, Nucl. Instrum. and Meth. B269 (2011)2413-2416.

[11] B. Rout, A.D. Dymnikov, D.P. Zachry, E.V. Eschenazi, Y.Q. Wang, R.R. Greco, G.A. Glass, Nucl. Instrum. and Meth. B261 (2007) 731–735.

[12] M. Oikawa, T. Satoh, T. Sakai, N. Miyawaki, H. Kashiwagi, S. Kurashima, S. Okumura, M. Fukuda, W. Yokota, T. Kamiya, Nucl. Instrum. and Meth. B260 (2007) 85–90.

[13] F.D. McDaniel, J.L. Duggan, C. Yang, B.N. Guo, M. El Bouanani, M. Nigam, Nucl. Instrum. and Meth. B181 (2001)99–103

[14] F. Nesprías, M. Venturino, M.E. Debray, J. Davidson, M. Davidson, A.J. Kreiner, D. Minsky, M. Fischer and A. Lamagna, Nucl. Instrum. and Meth. in Physics Research B267 (2009)69–73.

[15] Microbeam Scanning System - Installation and Operation Manual, Oxford Microbeams 1990

[16] J.L.Sanchez, J.A. van Kan, T. Osipowicz, S.V. Springham, F. Watt, Nucl. Instrum. and Meth. in Physics Research B136-138 (1998)385-389.

[17] A.A. Bettiol, J.A. van Kan, T.C. Sum, F. Watt, Nucl. Instrum. and Meth. in Physics Research B 181 (2001) 49-53.

[18] http://sine.ni.com/nips/cds/view/p/lang/en/nid/11310, NI PCI-6731 manual.

[19] D.N. Jamieson, G.J.F. Legge, Nucl. Instrum. Methods B 29 (1987) 544.

[20] D.N. Jamieson, G.J.F. Legge, Nucl. Instrum. Methods B 34 (1988) 411

[21] A. García-Navarro, A. Méndez, J. Olivares, G. García, F. Agullo-López, M. Zayat, D. Levy, L. Vázquez, Nucl. Instr. and Meth. B 257 (2007) 765.

[22] N. Fazzini, H. Gonzalez, S. Tau, A. Tersigni, Nucl. Instrum. and Meth. in Physics Research A268 (1988)330–333

Figure Captions.

Fig.1. The HiScan software graphical user interface is running under windows XP. The program was developed in LabView^{TM} environment. The figures represent the a) bottom, b) central and c) top shapes in which the MZ modulator pattern was divided to perform the high resolution vector scanning. Each part was specified by a file that contains up to a maximum of 10^4 points.

Fig. 2. PRAM simulations of single trajectories on x and y planes of $^{35}Cl^{6+}$ ions at 70 MeV energy from the object aperture of the microprobe, passing through the calibrated scanning system and the OM55 high strength quadrupole triplet. In the focusing plane, the beam is placed on the position for maximum deflection for both orthogonal axes, i.e. when the magnetic field strength of the scanning coils is maximized.

Fig. 3. PRAM simulation of three single particle trajectories in the x-plane with beam divergence $\phi_X \geq 75$ μrad. The ions with divergences -150 μrad $\leq \phi_X < 75$ μrad are deflected beyond the radius of the pipe lenses and do not reach the point focus. Note that the scanning length is approximately 4 mm.

Fig. 4. Comparison between the 3mm long cosine and double arc Y-branch shapes, with respect to the stretched shapes starting from an original 1mm length. The cosine shapes are overlapping, indicating that the cosine function is not modified by the stretching. In the amplified region, we show the portion with higher distance between the exact and uncorrected double-arc shapes. This difference is only 1.7% for a stretching factor of three.

Fig. 5. Optical micrograph of long lines produced in lithium niobate with a 5μm wide beam. (a) Average dose normalization. It can be seen as the line is vanishing as the scanning is reaching the end, (b) Pixel dose normalization. The machined line is extended in orther that the pixels of the extremes receive the right fluence.

Fig. 6. Profiles of induced Cu $K_{\alpha,\beta}$ X-ray yield as function of the $^{35}Cl^{6+}$ (70 MeV) beam position during a long horizontal scan. The open circles correspond to the average normalization curve which shows a sharp intensity decrease (and therefore of the fluence) at the ends of the scan. The open squares correspond to the X-ray yield for pixel normalization.

Fig. 7. Groups of micro-machined MZ shape arrays in $LiNbO_3$ with 1, 2 and 3mm length produced with a $^{35}Cl^{6+}$ at 70 MeV energy beam. Each array was written using only magnetic scan.

Fig. 8. a) Amplified image of one of the waveguide arms in the region of the contact electrodes. One can clearly distinguish the difference in resolution used en each scan. b) Shows a Y-branch for a 3mm long shape modulator in $LiNbO_3$ using a current of about 10 pA and a fluence of approximately 10^{13} ions/cm^2. The FWHM width of the channels is about 3.2 μm. The Y-branch corresponds to one end of the scan. The image shows no significant changes in the widths of the guides, showing that the beam focus is not affected by lens aberrations at the edges, at least, for the employed beam resolution.

Figure

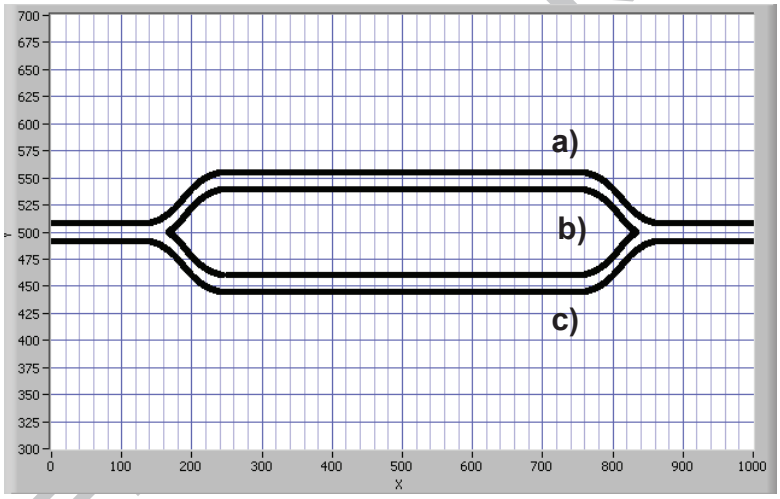

Figure

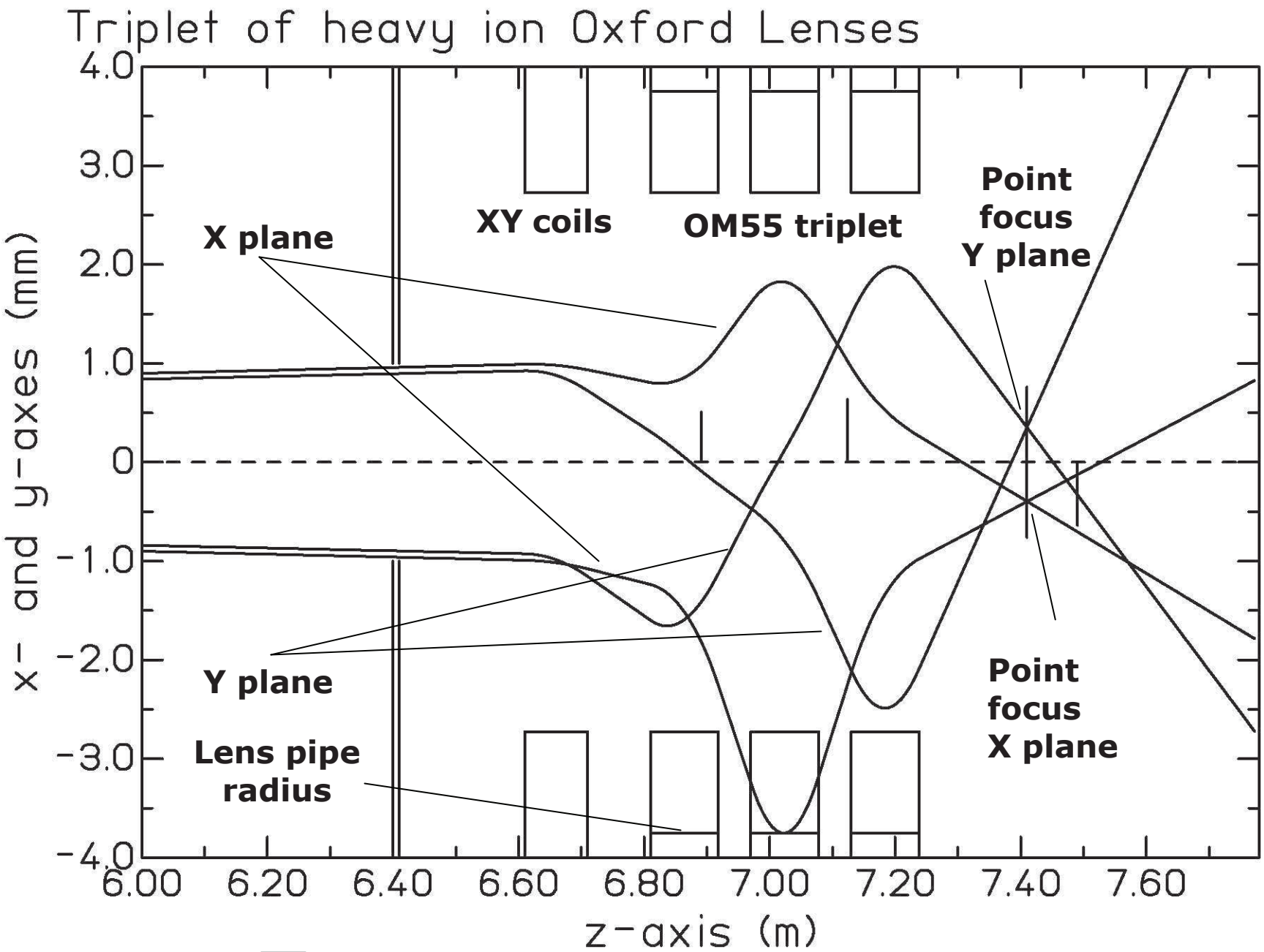

Figure

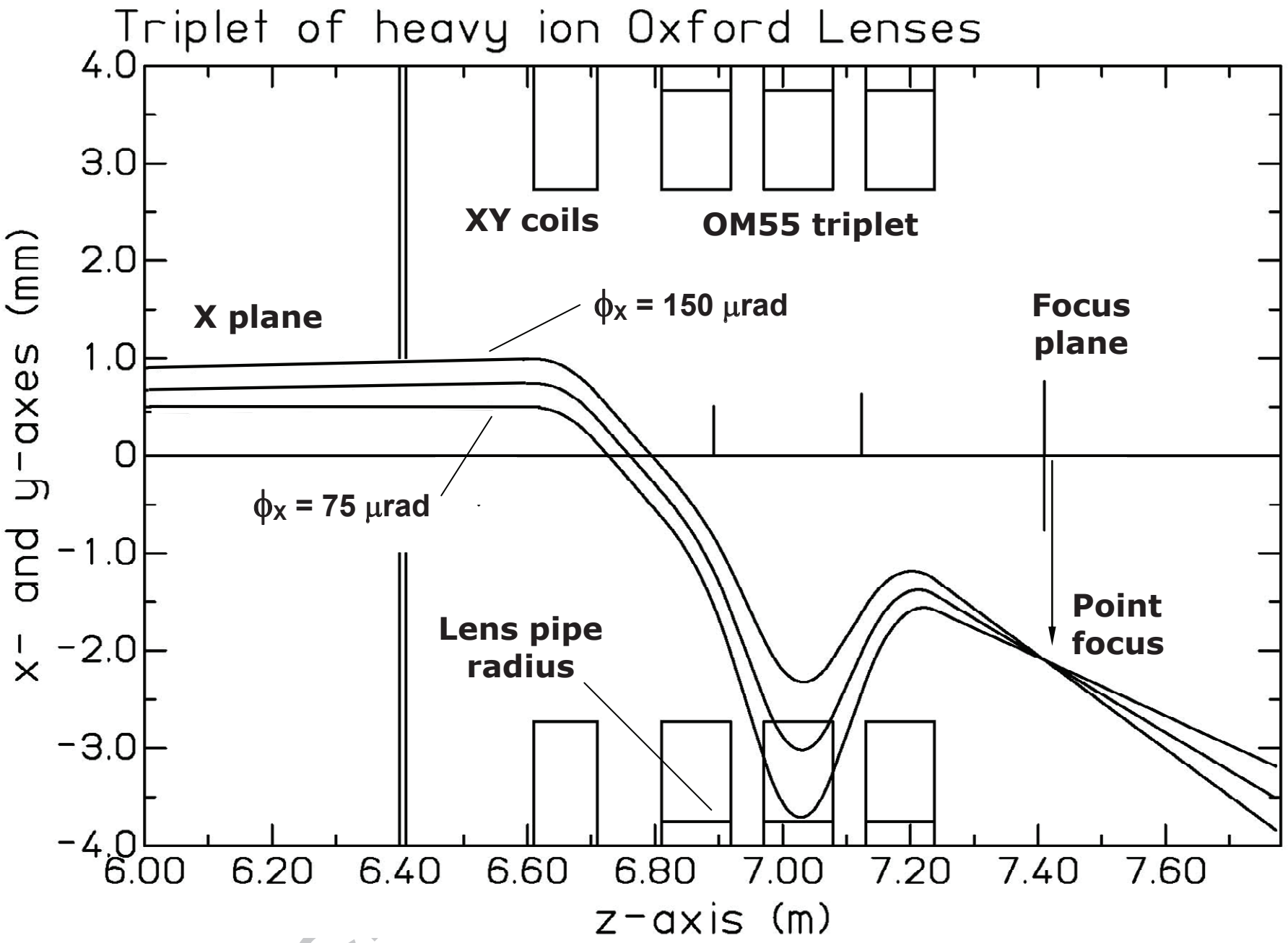

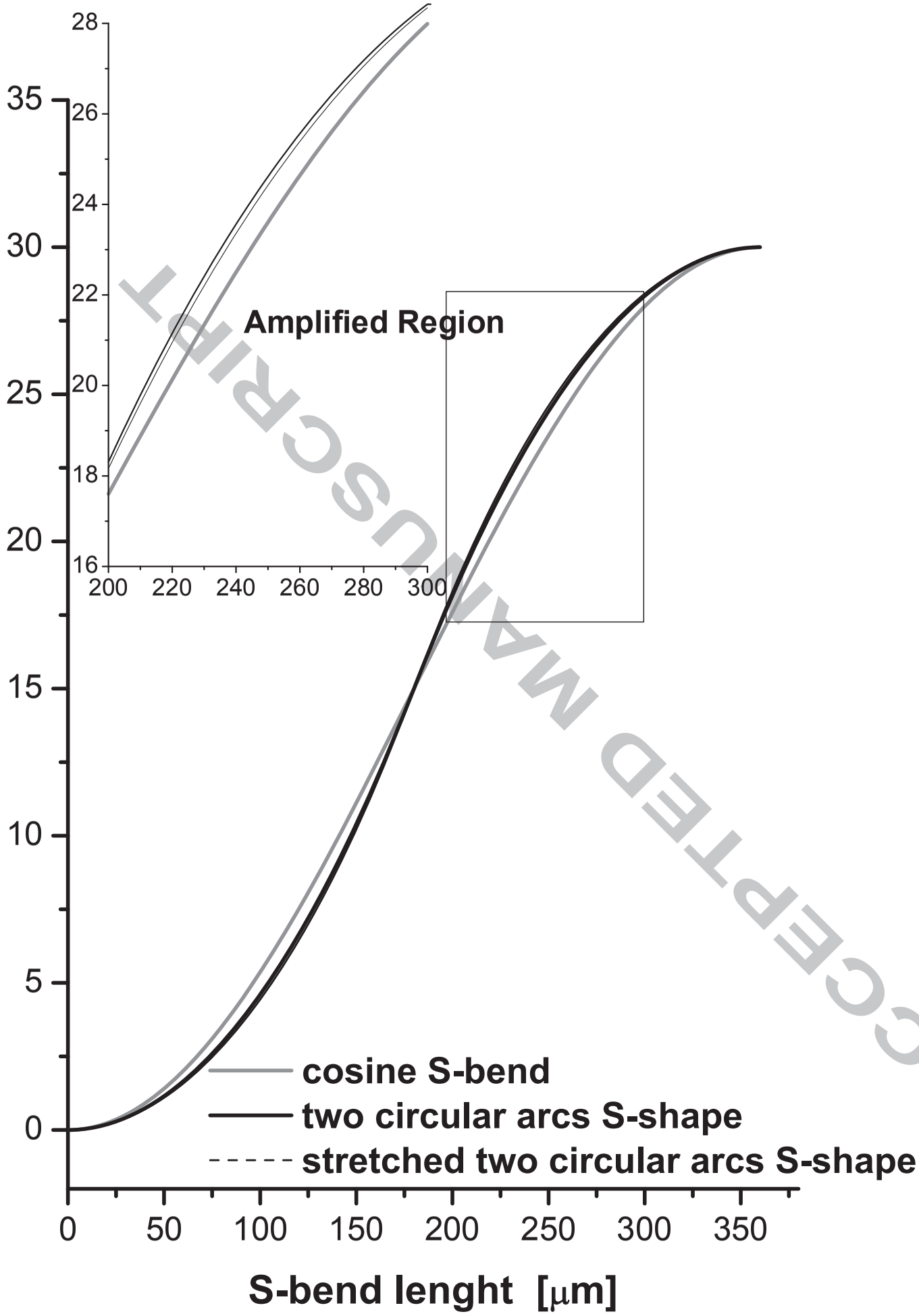

Figure

Figure

b

Figure

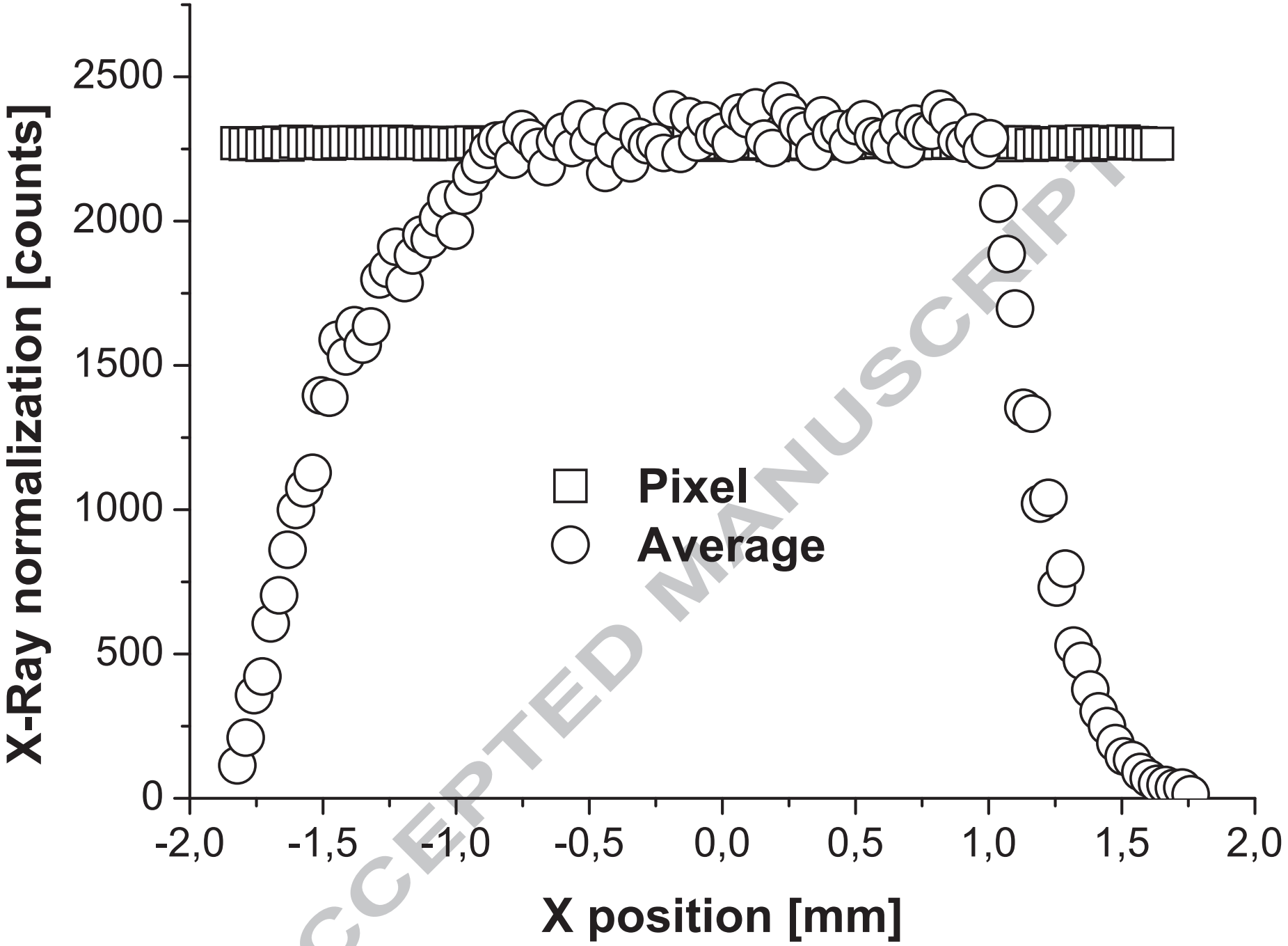

Figure

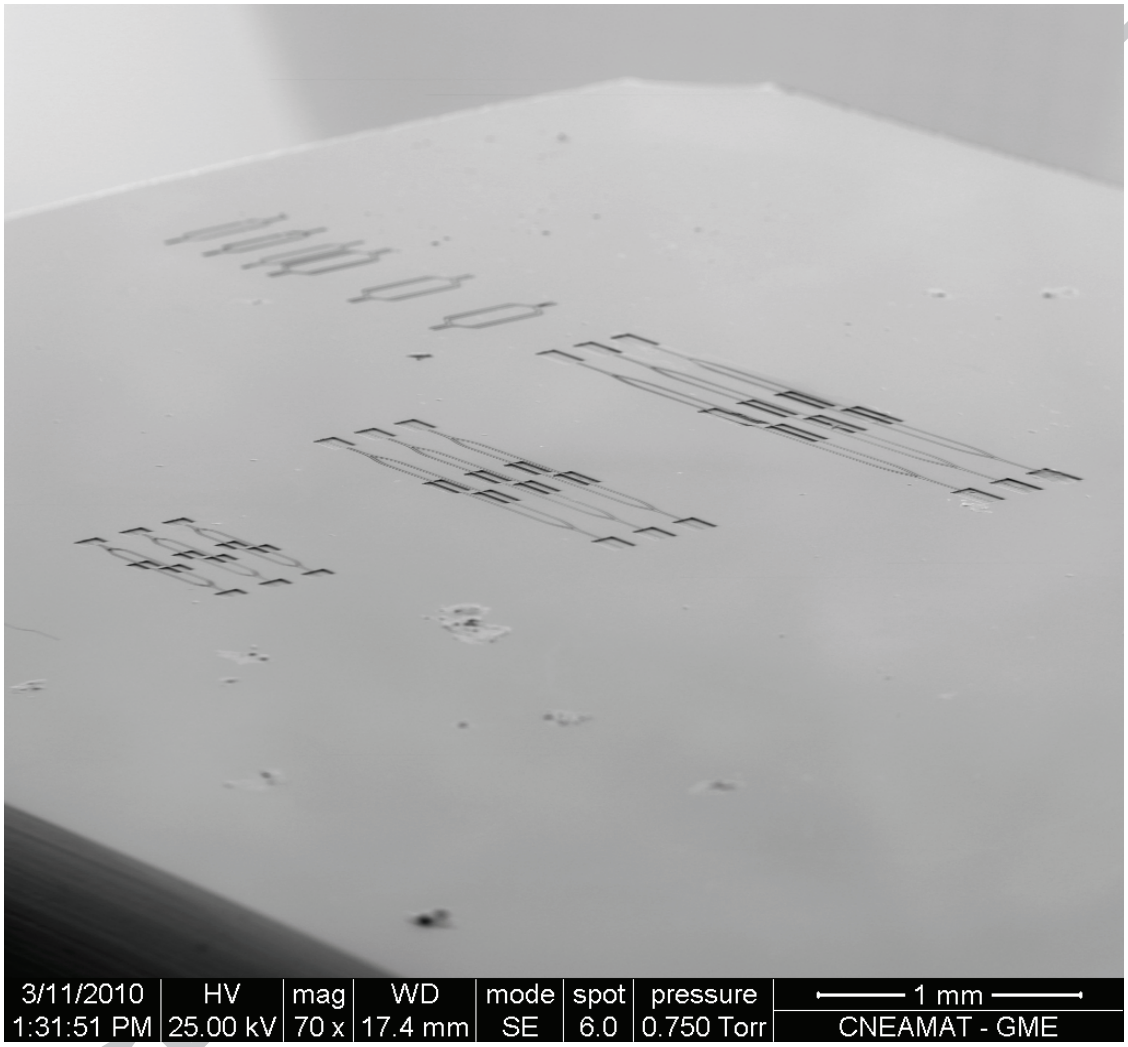

Figure